

TSUNAMI LOADING ON BUILDINGS WITH OPENINGS

P. Lukkunaprasit¹, A. Ruangrassamee² And N. Thanasisathit³

¹ Professor, Dept. of Civil Engineering, Chulalongkorn University, Bangkok, Thailand

² Assistant Professor, Dept. of Civil Engineering, Chulalongkorn University, Bangkok, Thailand

³ Ph.D. Student, Dept. of Civil Engineering, Chulalongkorn University, Bangkok, Thailand
Email: lpanitan@chula.ac.th, fcearr@eng.chula.ac.th, nutwut@gmail.com

ABSTRACT :

Reinforced concrete (RC) buildings with openings in the masonry infill panels have shown superior performance to those without openings in the devastating 2004 Indian Ocean Tsunami. Understanding the effect of openings and the resulting tsunami force is essential for an economical and safe design of vertical evacuation shelters against tsunamis.

One-to-one hundred scale building models with square shape in plan were tested in a 40 m long hydraulic flume with 1 m x 1 m cross section. A mild slope of 0.5 degree representing the beach condition at Phuket, Thailand was simulated in the hydraulic laboratory. The model dimensions were 150 mm x 150 mm x 150 mm. Two opening configurations of the front and back walls were investigated, viz., 25% and 50% openings. Pressure sensors were placed on the faces of the model to measure the pressure distribution. A high frequency load cell was mounted at the base of the model to record the tsunami forces.

A bi-linear pressure profile is proposed for determining the maximum tsunami force acting on solid square buildings. The influence of openings on the peak pressures on the front face of the model is found to be practically insignificant. For 25% and 50% opening models, the tsunami forces reduce by about 15% and 30% from the model without openings, respectively. The reduction in the tsunami force clearly demonstrates the benefit of openings in reducing the effect of tsunami on such buildings.

KEYWORDS: Tsunami loading, Building, Opening, Experiment, Pressure

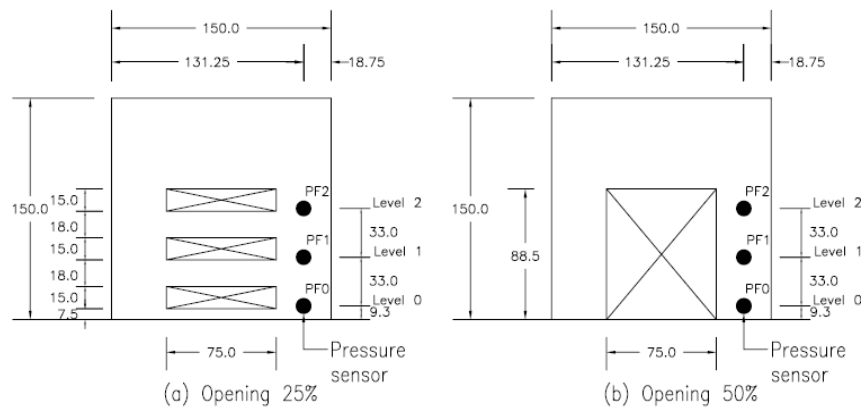


Figure 2 Configurations of the front and back panels of building model with sensor locations.



Figure 3 Formation of bore on slope beach (Nominal wave height = 80 mm)

3. Results

3.1. Velocity – Wave Height Relationship

The generated wave broke when approaching the beach at about 20 m upstream from the model, transforming into a bore before hitting the model (Figure 3). The typical time histories of the velocity of the wave and wave height at the location of the building model (in the absence of the model) are depicted in figure 4. It is to be noted that the leading edge of the wave attains a maximum velocity at the instant it reaches the location of interest when the wave height is still very small. As the wave increases in height, the velocity decreases significantly. Figure 5 shows the relationship between the measured maximum velocity of the leading wave front, V , and the maximum wave height, h . The associated peak wave velocities generated varied from $2.4\sqrt{(g*h)}$ - $3.0\sqrt{(g*h)}$, where g is the acceleration due to gravity. In the absence of a laboratory test, it is not known in advance the value of V corresponding to a particular value of wave height. Thus, it is for convenience to express the maximum velocity in terms of the maximum wave height.

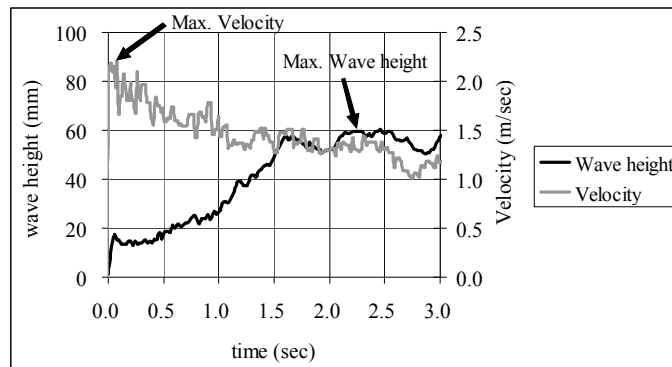


Figure 4 Typical time history records of wave height and velocity at location considered (without structure) - nominal wave height = 60 mm

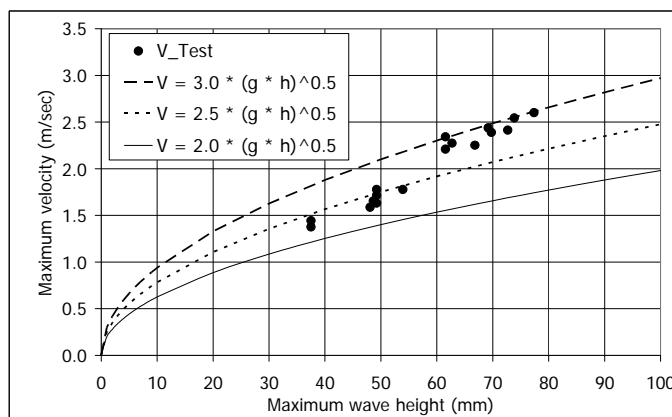


Figure 5 Relation between maximum velocity (V) and the maximum wave height (h)

3.2. Model Without Openings

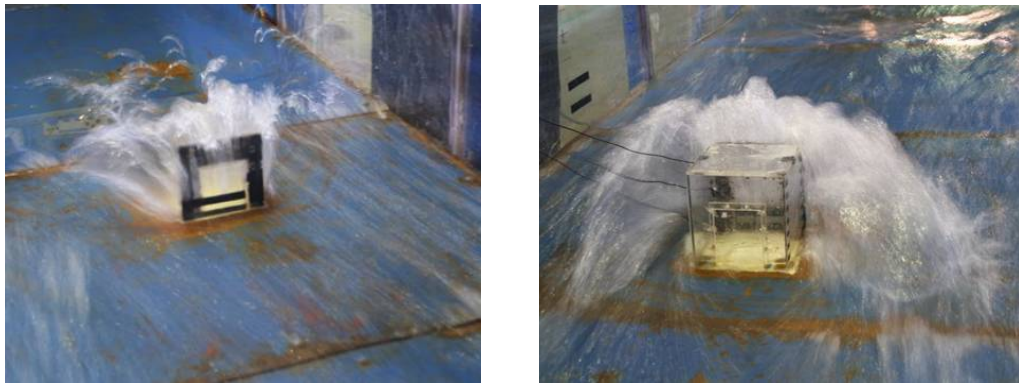
When the leading edge of the wave hit the model, the wave splashed up its front face much like a wave striking a wall as depicted in the photo shown in figure 6. However, the energy imparted to the structure in the case of the 3-dimensional model was considerably less than that on a 2-dimensional wall (taller than the splash-up height) since part of the splash was diverted sideways upon impact, and part of it overtopped the model for the cases of 60 and 80 mm nominal wave heights with the splash reaching more than 2 times the model height. No overtopping occurred for the 40 mm wave height.

Figure 7 depicts typical time records of the pressures at the upstream face of the building model without openings. As expected, one may note the high impact pressure at impingement of the leading tongue upon the model. Figure 8 shows the typical normalized pressure on the solid model (without openings) at different instants of time, corresponding to the attainment of peak pressure readings at different levels. The pressure distribution at the instant the wave force is maximum is also shown in the figure. It is noted that upon impingement of the leading tongue on the model, the pressure at the bottommost sensor (located at 9 mm above the base) attains a very high value of more than 4 times the hydrostatic pressure, and the pressure concentrates over approximately half the maximum wave height. As time progresses, the peak pressure near the base decreases while the values increase at higher levels. At the instant the wave force on the model is maximum, the peak pressure drops to about 2.4 times the hydrostatic pressure. The pressure profile associated with the maximum wave force can be conservatively approximated by a bi-linear distribution shown in Figure 8 with a value of 2.75 times the hydrostatic pressure over one wave height above the base and decreasing to zero at 2 times the inundation height. The pressure, p_i , at height z can thus be expressed as follows:

$$p_i / \rho gh = \begin{cases} 5.5 - 2.75z/h & \text{for } z/h > 1 \\ 2.75 & \text{for } z/h \leq 1 \end{cases} \quad (3.1)$$

where ρ is mass density of water.

It should be noted that designing the building using the pressure profile envelop would significantly overestimate the actual peak force exerting on the structure.



(a) front view (b) rear view
 Figure 6 Snapshots of flow past the model at impact

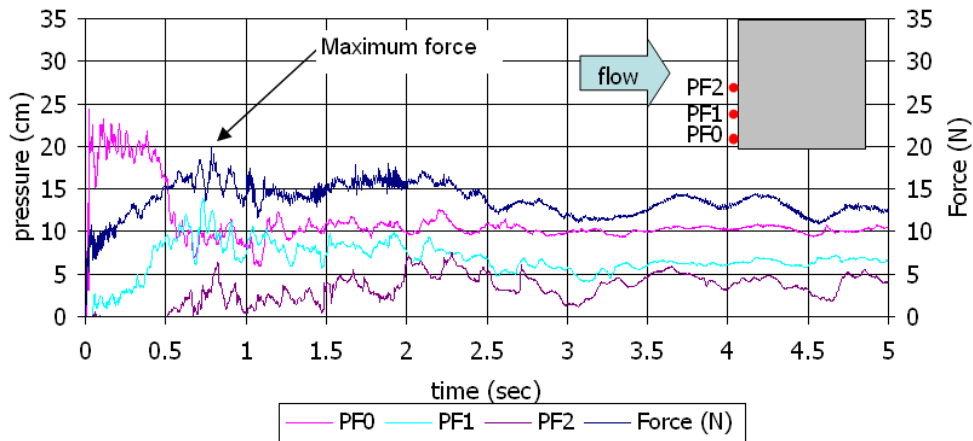


Figure 7 Typical time records of the pressures at the upstream face of the building model without openings

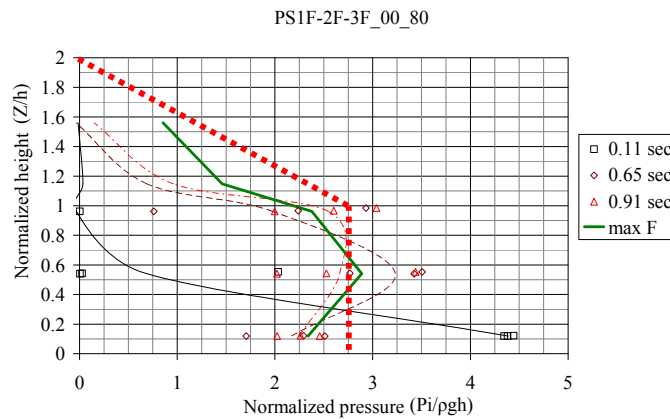


Figure 8 Typical normalized pressure at different instants of time at different levels
 (Nominal wave height = 80 mm)

The wave force-height curve computed based on the proposed pressure profile is practically the upper bound curve for the experimental results as depicted in the figure 9. Also shown in the figure are the hydrodynamic forces (drag forces) determined in accordance with FEMA 55 (2000) guidelines based on the maximum wave velocity measured from the experiments. It may be noted that the calculated drag forces on the model are, in general, larger than the experimental values by 12%- 44%.

Square model without openings, Kamala, Phuket

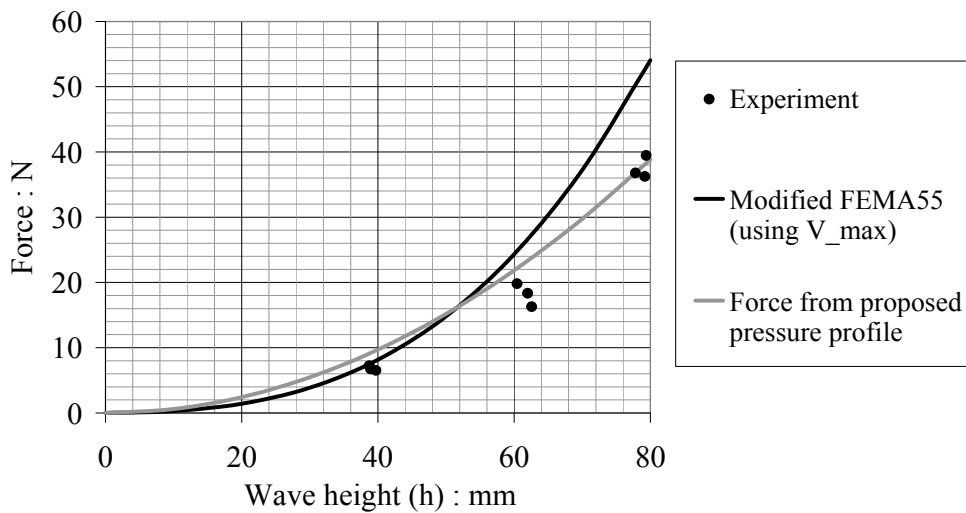


Figure 9 Comparison of tsunami forces obtained from experiments with those based on FEMA-55 guidelines and the proposed pressure profile.

3.3. Effects of Openings

The influence of the openings on the peak pressures on the front panel of the model is found to be practically insignificant as can be seen in Table 1.

Table 1 Normalized pressure ($P_i/\rho gh$) at positions PF0, PF1 and PF2 – square model with different openings

Opening	Nominal Wave height								
	40 mm			60 mm			80 mm		
	PF0	PF1	PF2	PF0	PF1	PF2	PF0	PF1	PF2
0%	2.65	1.23	0.49	3.96	2.08	1.11	4.36	3.10	2.30
25%	2.80	1.04	0.33	4.56	2.04	1.19	4.61	2.71	2.14
50%	2.99	1.16	0.13	4.94	1.93	1.26	4.66	3.07	2.40

Note: PF0, PF1 and PF2 denote pressure sensor on the front face of model at levels 9.3 mm, 42.3 mm and 75.3 mm above the base, respectively.

Table 2 shows the variation of tsunami force, F_s , on the model with wave height for various opening configurations. It should be noted that F_s is the wave force acting on the whole structure and, for the case of models with openings, it includes the forces exerted by the wave on both the front and back panels of the model. Since the pressures on the upstream face of the model is not significantly affected by the presence of openings as discussed earlier, the reduction of the tsunami force on the upstream panel may be taken as proportional to the reduction in the panel area by the openings. Thus, for the case of 50% opening, in the absence of test results one may have to approximate the total force F_s to be equal to that acting on a solid model (without opening). However, as evidenced in the test results in table 2, F_s decreases by about 30-40% in comparison with the solid model. The corresponding reduction is about 15-25% for the case of 25 % opening.

Table 2 Tsunami force (N) on square model with different opening configurations

Opening	Nominal Wave height		
	40 mm	60 mm	80 mm
00%	6.8 (100%)	18.1 (100%)	37.9 (100%)
25%	5.1 (75%)	15.5 (85%)	31.5 (83%)
50%	4.3 (63%)	11.2 (62%)	26.2 (69%)

Note: Values in parentheses are percentage of the model without openings

4. CONCLUSIONS

Based on the experimental data of the pressure distributions on the face of the square building model without openings at various instants of time, a simplified bi-linear pressure profile is proposed for determining the maximum tsunami force acting on the structure, with the resulting force - wave height relation bounding the experimental results. The presence of openings allows water to enter the building, creating counteracting pressure on the inside of the upstream panel. Moreover, there exists a shielding effect which reduces the force acting on the rear panel. The tests show that there is a reduction in the wave force acting on the whole building in the order of 15% - 25% for the 25% opening configuration, and 30% - 40% for case of 50% opening. The corresponding reduction for the force on the front panel based on pressure recordings can be assumed to be 25% and 50%, respectively. The reduction in the tsunami force clearly demonstrates the benefit of openings in reducing the effect of tsunami on such buildings.

ACKNOWLEDGMENTS

The funding from the Department of Public Works and Town and Country Planning, Ministry of Interior and The Royal Golden Jubilee Project of the Thailand Research Fund is gratefully acknowledged. The support of Chulalongkorn University and the Asian Institute of Technology is highly appreciated. The authors greatly appreciate the valuable contributions of Prof. T. Takayama and Assoc. Prof. Pennung Wanitchai. The assistance of Dr. Somboon Siangchin and Mr. Surakai Banchuen is also acknowledged.

REFERENCES

- Asakura, R., Iwase, K., Ikeya, T., Takao, M., Kaneto, T., Fuji, N., and Ohmori, M. (2002). The Tsunami Wave Force Acting on Land Structures. *Proceedings of the 28th International Conference on Coastal Engineering*, 1191-1202.
- Cross, R.H. (1967). Tsunami surge forces. *Journal of the Waterways and Harbors Division, Proceedings of the American Society of Civil Engineers* **93:WW4**, 201-231.
- FEMA (2000). Coastal Construction Manual, FEMA 55 Report, Federal Emergency Management Agency, Washington, D.C.
- Fukui, Y., Nakamura, M., Shiraishi, H., and Sasaki, Y. (1963). Hydraulic Study on Tsunami. *Coastal Engineering in Japan, The Japan Society of Civil Engineers*, Tokyo **6**, 67-82.
- Hamzah, M.A., Mase, H., and Takayama, T. (2000). Simulation and Experiment of Hydrodynamic Pressure on a Tsunami Barrier. *Proceedings of the 27th International Conference on Coastal Engineering*, 1501-1507.
- Lukkunaprasit, P. and Ruangrassamee, A. (2008). Building Damage in Thailand in 2004 Indian Ocean Tsunami and Clues for Tsunami-Resistant Design. *The Institution of Engineers Singapore Journal, Part A: Civil and*

Structural Engineering **1:1**, 17 – 30.

Ramsden J. D. (1996). Tsunamis forces on a vertical wall caused by long waves, bores, and surge on a dry bed. *Journal of Waterway, Port, Coastal, and Ocean Engineering* **122:3**, 134-141.

Ramsden J. D. and Raichlen F. (1990). Forces on vertical wall caused by incident bores. *Journal of Waterway, Port, Coastal, and Ocean Engineering* **116:5**, 592-613.

Yeh, H. (2007). Design tsunami forces for onshore structures. *Journal of Disaster Research* **2:6**, 531-536.